SECRET

RESTRICTED DATA

ATOMIC ENERGY ACT - 1954

AFSWP—1069

U S AIR FORCE

PROJECT RAND

RESEARCH MEMORANDUM

A NEW MODEL FOR FALLOUT CALCULATIONS (U)

R. R. Rapp

RM-2115

13 February 1958

Copy No.______

Assigned to ________________________

DISTRIBUTION RESTRICTIONS

Not suitable for distribution to foreign governments or foreign nationals.

Not suitable for distribution to industrial contractors or commercial organizations.

[redacted]

The RAND Corporation

1700 MAIN ST. • SANTA MONICA • CALIFORNIA

SECRET

distributions.

The Zuni rockets passed very nearly over ground zero and therefore were assumed to represent a vertical plane through the diameter of the cloud. In order to further simplify the problem circular symmetry about ground zero will be assumed. The data were then plotted at the appropriate height and distance from ground zero and smooth contours of the reported rocket readings were drawn (Fig. 5).

From the smoothed contours, the total activity in the cloud was computed by a numerical integration. From the total activity and the smooth contours, the fraction of activity per cubic kilofoot was computed as a function of height and radial distance is shown in Table 2.

The estimate of $A_2(H)$ was chosen as the marginal distribution which is obtained from the numerical integration of R A(R,H) dR at several different heights. This distribution is shown in Fig. (6). The estimate of $A_3(R)$ was chosen as the integration of A(R,H) dH for several different values of R. Figure (7) shows this distribution.

The distribution of activity with particle size was chosen as the distribution presented in reference (1). Accumulative distribution was plotted; points were read from the cumulative function; and numerical differentiation was used to determine values of $A_1(r)$. Since this is a badly skewed distribution, it is convenient to use as a variable ln(r) instead of r. Figure (8) shows the activity as a function of size for this distribution.

RM-2115
2-13-58
22

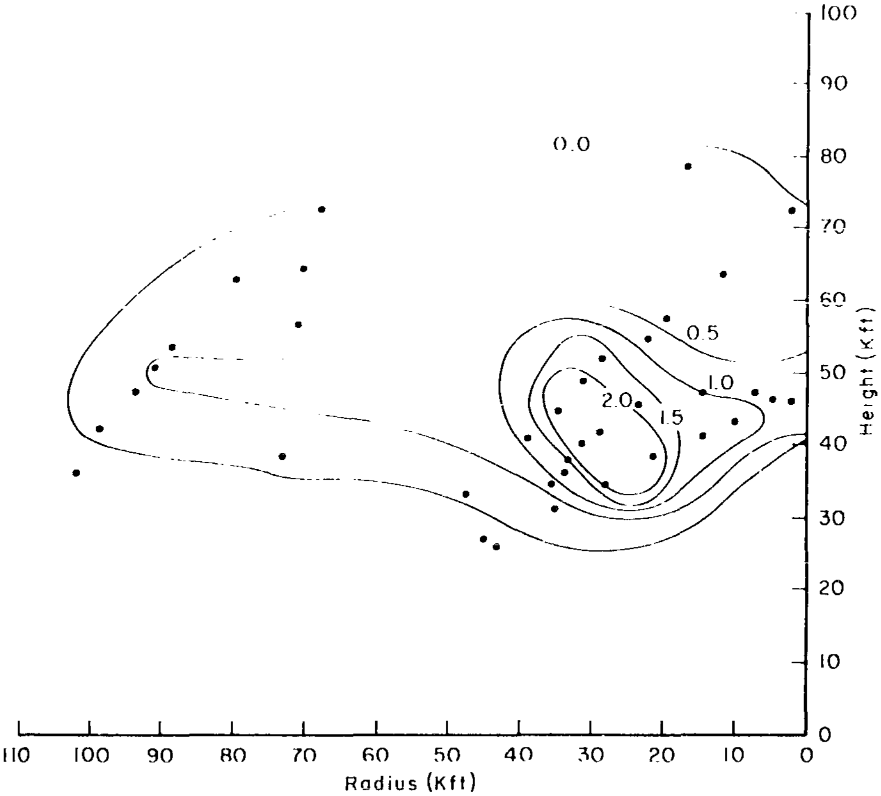

Fig. 5—Results of Zuni rocket measurements (a) at 7 min with subjective isopleths

Table 2

Debris Concentration (Fraction per Cubic Kilofoot x 10^5) from Rocket Results as a Function of Radius and Height

Height (kft)	Radius (kft)									
	5	15	25	35	45	55	65	75	85	95
5										
15										
25										
35		1.223	2.751	1.528	.489	.122				
45	.856	1.528	2.45	3.056	1.467	.795	.672	.672	.587	.489
55	.538	.562	1.223	1.589	.917	.611	.562	.550	.599	.306
65	.245	.306	.367	.428	.367	.306	.245	.061		
75	.061	.183	.245	.183	.122	.122				

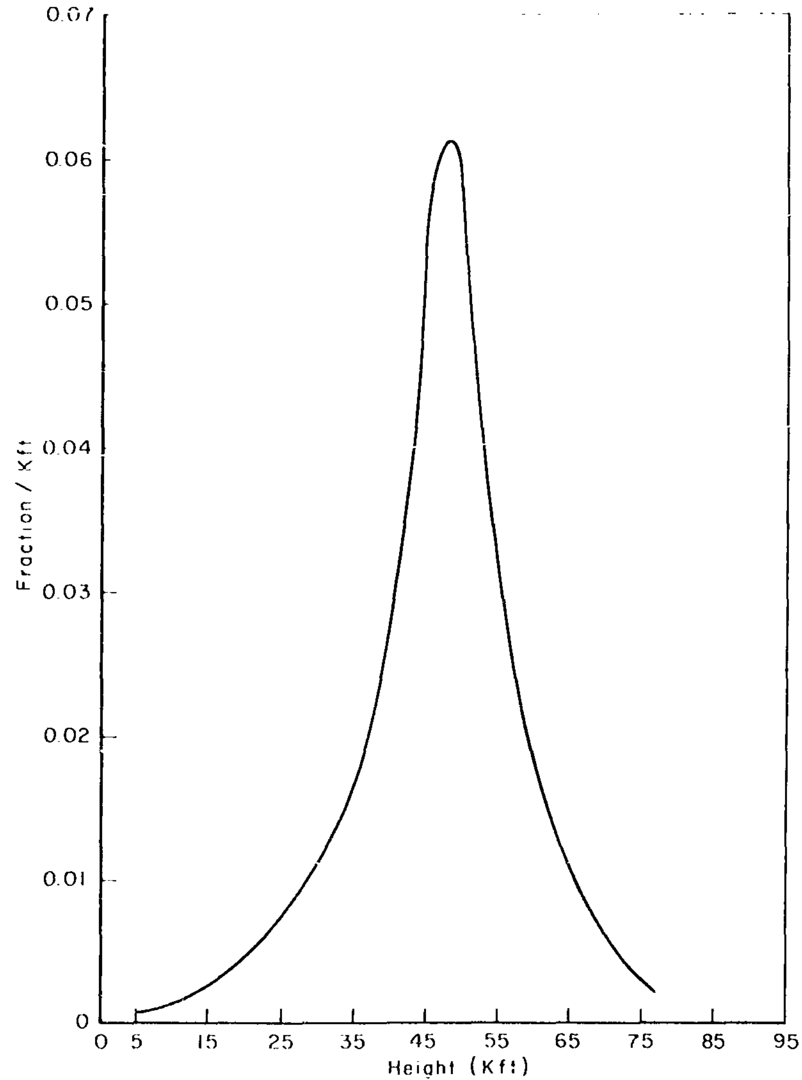

Fig. 6—Smoothed distribution of activity with height from Zuni rocket data

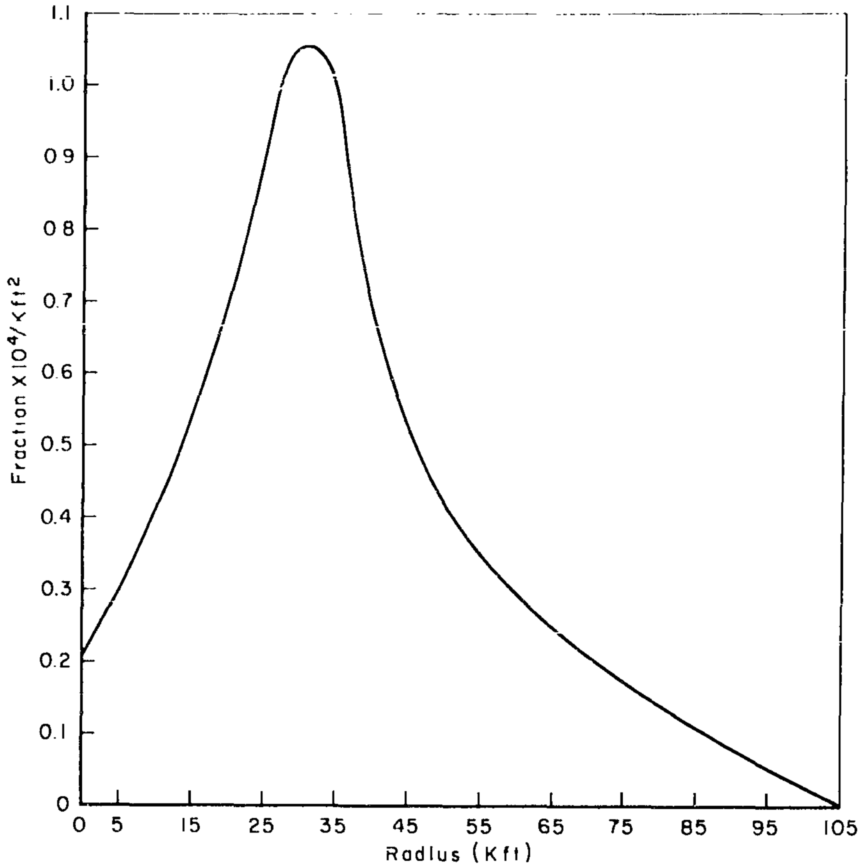

Fig. 7—Smoothed distribution of activity with radial distance from the cloud center from Zuni rocket data

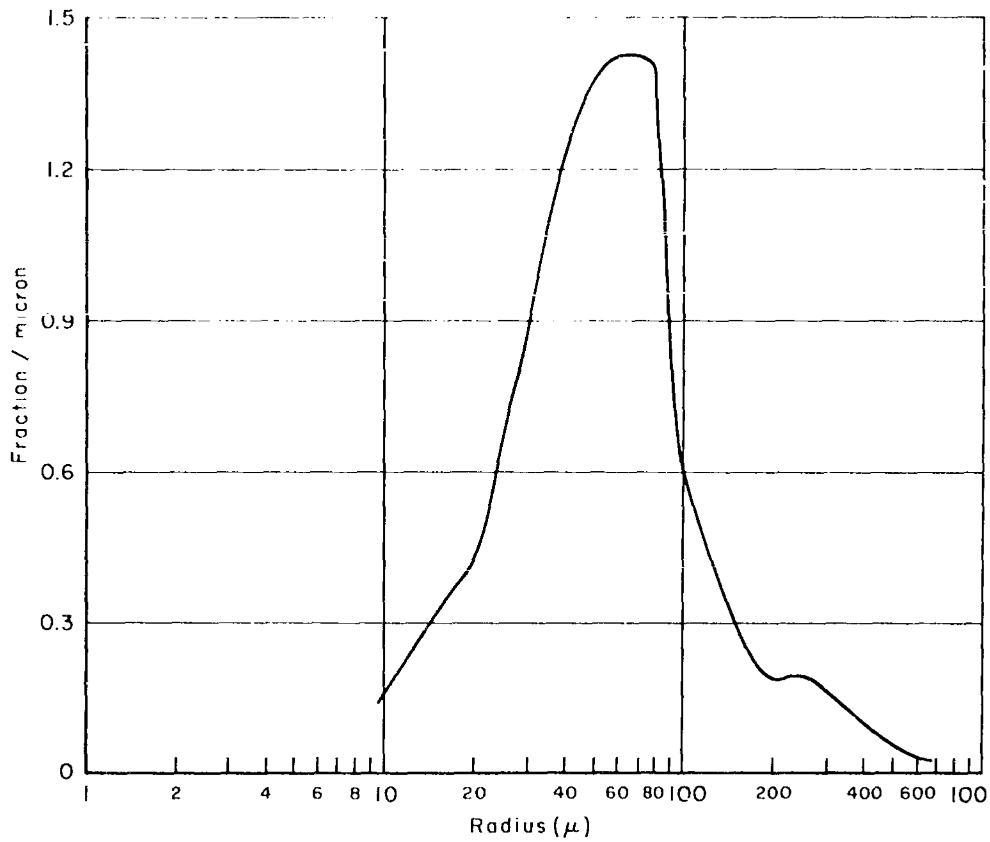

Fig. 8—Fraction of activity per micron as a function of radius of particle

IV. DISCUSSION

The initial test of the model, which will be referred to as "run 1," was made with the Castle-Bravo wind data taken from Dean and Ohmstead. The details are presented in the Appendix.

The ground position of a few selected particles, which were read from the results of the meteorological part of the computation, are shown in Fig. (9), which also shows the circular standard errors, derived from the discussion of meteorological errors, with the assumption of an error standard deviation, σ_{ϵ} , equal to 5 knots. It appears, from this figure, that random errors of this magnitude will not produce large errors in the orientation and general configuration of the pattern. It does seem reasonable to assume, however, that this type of error may cause a considerable error in the fraction of fallout at some point near the boundary of the fallout area. It must be emphasized that these wind error estimates do not include any gross error in defining the vector wind field.

Several variations of the activity functions were tried with the basic wind pattern of run 1. The purpose of these calculations was to make some qualitative estimates of the effect of changing the distribution functions. The details of these calculations are given in the Appendix and are referred to as run 1a, 1b, etc. The inferences which may be drawn from an inspection and comparison of the results of the calculations will be taken up in order.

The difference between runs 1a and 1b was only in the $A_1(r)$ function. The function used in 1b was a log-normal distribution with the same mean and standard deviation as the distribution shown in Fig. (6). The difference between the patterns is not striking. The 1b pattern is not as intense at the hot spot as the 1a pattern, but this was expected since the 1b pattern

SECRET
RESTRICTED DATA
ATOMIC ENERGY ACT 1954

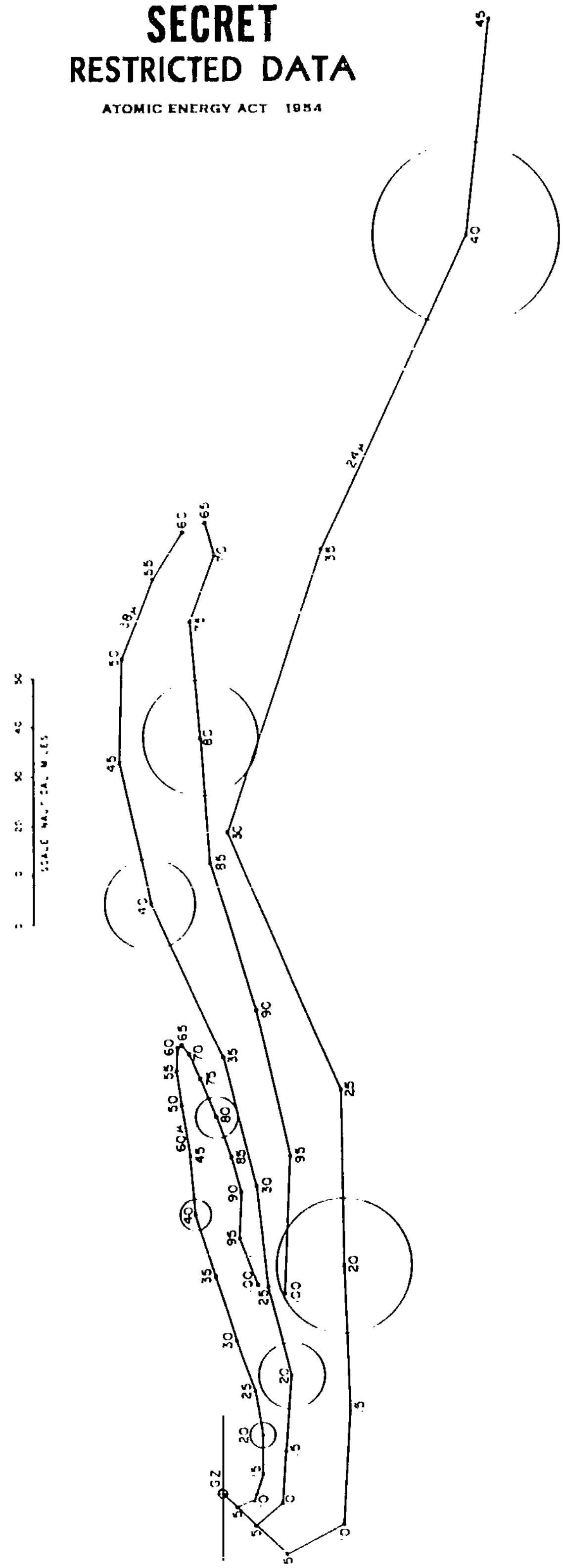

Fig. 9—Ground position and circular standard errors of selected particles

SECRET

had less material concentrated near the mean.

A comparison of runs a and b shows several interesting facts. The largest change is about 30 per cent at the point of maximum deposition in both of the patterns. The log-normal distribution of run 1b has fewer particles in the size below 55μ than does the RAND distribution of run 1a. The distribution used in run 1b also shows a higher close-in value than does the run 1a, indicating too much activity on larger particles.

A comparison of both of these runs with the fragmentary data of the Castle-Bravo shot brings two facts to light. The first point is that both the 1a and 1b distributions show far too large a fraction on the islands of the Bikini Atoll. The second point is that values are low in the northern part of Rongelap.

These errors may be due to an incorrect wind analysis, but they could also be explained by a set of incorrect distribution functions. In any event, the relatively slight change in the patterns between an empirical distribution and a mathematical model seems to be slight. This suggests that an attempt could be made to fit the best possible log-normal, or any other useful function, to the existing data.

Runs 1c and 1d were made to note the comparison of the old model with the new. Run 1c was the mushroom portion, and run 1d was the stem; together they reproduce a pattern with essentially the same assumptions as the old RAND model. The pattern for run 1c, the mushroom portion, again shows relatively slight differences from runs 1a and 1b. The addition of the stem material from run 1d makes little change in the pattern. The greatest contribution from the stem is near ground zero, which is already too high, and near the perimeter of the pattern where the uncertainty is greatest.

A rather drastic change in the distribution of activity with size was made in run 1e. The amount of activity on particles greater than 95μ radius was halved, and this excess was added to the particles between 35μ and 65μ in radius. This run used the same spatial distribution as runs 1a and 1b. The "hotspot" for run 1e was moved far away from ground zero and was reduced in intensity.

V. CONCLUSIONS

Since the observations on Castle-Bravo were fragmentary, there is no useful purpose to be served by continuing variation of parameters on the set of winds from this shot. The work done has proven the feasibility of the approach and has verified the accuracy of the model within the limits of the available data. It is believed that the next set of data processed can proceed on the assumptions that:

1. small changes in the distribution functions will produce only negligible changes in the pattern;

2. the wind patterns are sufficiently accurate to put limits on the possible distribution functions;

3. the gross effects of the fallout from large-yield shots are not affected by stem material.

It may be inferred that most of the material is lodged on particles in a very narrow range of sizes and that it is concentrated into a very narrow range of heights at the time of stabilization.

The next set of runs will be made on the Zuni shot of Operation Redwing. An attempt will be made to adjust the distribution functions so as to produce calculated values of the fraction-down which are within the range of error measurement at those stations for which adequate measurements are available. This then will be assumed to be the optimum model, and the errors of this model will be assumed to be a minimum for fallout calculations.

APPENDIX

A. METEOROLOGICAL DATA

Run 1 refers to those fallout calculations that were based on the winds at the time of the Castle-Bravo event. The winds were read from the Dean and Ohmstead charts at 8 locations. Table A1 gives these locations in terms of N-S and E-W distances from ground zero. It was necessary to insure that there were no three points which could be simultaneously colinear and closest to the falling particle, because this situation would invalidate the interpolation functions. The winds were read at two different times (8.25 hours and -15.75 hours from H hour). For times longer than 8.25 hours the wind was assumed to be invariant with time. Table A2 lists the winds at the eight points at two different times.

Table A1

Positions of Points, Relative to Ground Zero, Where Wind Information was a Machine Input

Point	Distance East (n mi)	Distance North (n mi)
A	-14	50
B	136	50
C	286	100
D	436	50
E	-14	-100
F	136	-100
G	286	-50
H	436	-100

Table A2a

Wind Values for Run 1
at 15.75 Hours before Shot Time

Elevation (ft)	Position*															
	A		B		C		D		E		F		G		H	
	V	α	V	α	V	α	V	α	V	α	V	α	V	α	V	α
5,000	07	45	09	52	09	92	10	85	09	75	13	55	14	254	10	040
10,000	18	305	11	330	13	170	12	130	15	265	10	310	05	350	05	290
15,000	12	265	11	280	13	214	8	210	12	248	10	289	07	297	09	250
20,000	16	220	17	250	18	240	18	250	10	220	12	270	13	230	14	250
25,000	22	233	23	250	23	243	24	250	16	226	17	238	15	255	20	241
30,000	28	240	29	250	29	245	29	250	22	230	25	225	20	240	25	235
35,000	28	244	29	254	30	253	32	257	22	233	25	233	21	249	27	247
40,000	27	250	29	258	31	259	35	264	23	237	25	241	24	253	29	256
45,000	27	255	30	262	33	265	39	266	24	242	26	248	27	255	33	254
50,000	27	260	30	265	35	270	42	270	24	245	27	255	30	270	37	270
55,000	20	264	22	269	25	274	33	273	16	246	18	259	20	275	27	273
60,000	12	265	24	278	18	283	23	279	08	250	11	268	13	236	17	279
65,000	02	285	08	302	11	302	14	294	01	349	02	310	07	330	08	299
70,000	03	50	07	08	08	335	08	335	09	54	07	42	08	025	06	025
75,000	12	67	12	42	13	40	12	35	17	59	15	56	15	30	14	062
80,000	20	70	20	55	20	55	20	55	25	60	23	60	22	60	23	70

* V = Speed (kn)
α = Direction (10's of degrees from N)

Table A2b

Wind Values for Run 1
at 8.25 Hours after Shot Time

Elevation (ft)	Position* A		B		C		D		E		F		G		H	
	V	α	V	α	V	α	V	α	V	α	V	α	V	α	V	α
5,000	09	015	06	110	06	100	08	088	09	062	08	075	10	070	09	064
10,000	12	340	10	270	07	280	06	320	10	270	05	230	05	330	05	315
15,000	16	303	14	283	12	302	11	317	13	277	08	304	09	343	06	317
20,000	23	285	19	290	17	310	17	315	17	280	16	320	13	340	10	320
25,000	29	275	25	271	20	271	16	265	18	244	15	264	11	250	13	23[illegible]
30,000	35	270	34	250	30	250	29	230	25	220	25	230	25	220	25	215
35,000	40	264	41	260	39	253	38	246	32	220	33	236	33	233	30	236
40,000	45	260	46	250	49	255	49	255	39	220	42	240	42	240	39	250
45,000	38	266	44	265	45	266	48	268	23	212	23	251	29	262	37	273
50,000	32	275	40	270	43	275	50	280	10	180	10	310	25	300	41	295
55,000	19	276	24	270	27	272	32	275	03	214	08	288	17	285	27	284
60,000	06	280	08	270	12	260	15	260	07	330	08	260	12	260	17	250
65,000	04	014	03	345	11	288	06	278	08	039	02	044	03	315	05	296
70,000	11	050	09	046	07	005	06	034	15	062	11	066	10	055	10	042
75,000	18	057	17	057	15	050	16	055	24	071	21	069	20	065	22	055
80,000	25	060	25	060	25	060	25	060	32	075	30	070	30	065	34	060

*V = Speed (kn)
α = Direction (10's of degrees from N)

B. GEOMETRIC DATA

Run 1a

In order to adjust the geometric distribution functions A_2 and A_3 to to the yield of the Castle-Bravo event, it is necessary to spread the debris over a larger region of space. Since the integrals of the A functions must equal 1, the actual activities must be reduced accordingly. According to Kellogg[10] the cloud diameter of a 3.5 MT device is ~20 n mi and a 15 MT device is ~ 29 n mi. Since the Zuni distribution of $A_3(R)$ reduced to nearly zero at ~17 n mi (see Fig. 8), it was scaled up to ~24 n mi for the Castle-Bravo shot. The activity A_3 was therefore reduced. In a similar way the height of the cloud was increased, and the activity fraction A_2 was decreased.

All of the values of A were tabulated to such a degree that linear interpolation caused less than 1 per cent in the difference between the curves and the interpolated values. The tabulated distribution functions are shown in Table A3.

The machine output gives the fraction of device per square kilofoot at a number of pre-chosen points. The results of this calculation for run 1a are shown in Fig. A1. The isopleths that are drawn on Fig. 9, are subjective estimates of the lines of equal fraction down.

Run 1b

The conditions for run 1b are the same as for run 1a except for the distribution of activity with particle size. The distribution used in run 1b is the log-normal distribution with the same mean and standard deviation as the distribution in run 1a. Table A4 shows the values of $A_1(r)$ as a function of r and also the differences between $A_1(r)$ for run 1a and $A_1(r)$

Table A3

Activity Function for Run 1a

h (kf)	$A_2(H)$	r(μ)	$A_1(\ln r)$	R(n mi)	$A(R) \times 10^{-4}$
0	0	9.5	0.15	0	.102
5	.00024	12.25	0.24	.822	.138
10	.00068	15.0	0.33	1.645	.174
15	.00140	20.0	0.41	2.467	.211
20	.00240	24.0	0.66	3.289	.260
25	.00376	31.0	0.93	4.112	.316
30	.00544	38.0	1.19	4.934	.385
35	.00760	49.0	1.37	5.757	.456
40	.01040	60.0	1.42	6.579	.688
45	.01464	77.5	1.41	7.401	.764
50	.02200	95.0	0.68	8.224	.495
55	.03560	123.0	0.43	9.046	.372
60	.04904	151.0	0.27	9.868	.303
65	.03624	195.0	0.19	10.691	.252
70	.00280	239.0	0.20	11.513	.218
75	.01456	309.0	0.16	12.336	.191
80	.00976	379.0	0.11	13.158	.169
85	.00632	489.0	0.06	13.980	.151
90	.00384	600.0	0	14.803	.131
95	.00208			15.625	.117
100	.00128			16.447	.102
				17.270	.089
				18.092	.076
				18.914	.065
				19.937	.054
				20.559	.044
				21.382	.033
				22.204	.023
				23.026	.014
				23.849	.005

RM-2115
2-13-58
38

SECRET

RESTRICTED DATA

ATOMIC ENERGY ACT 1954

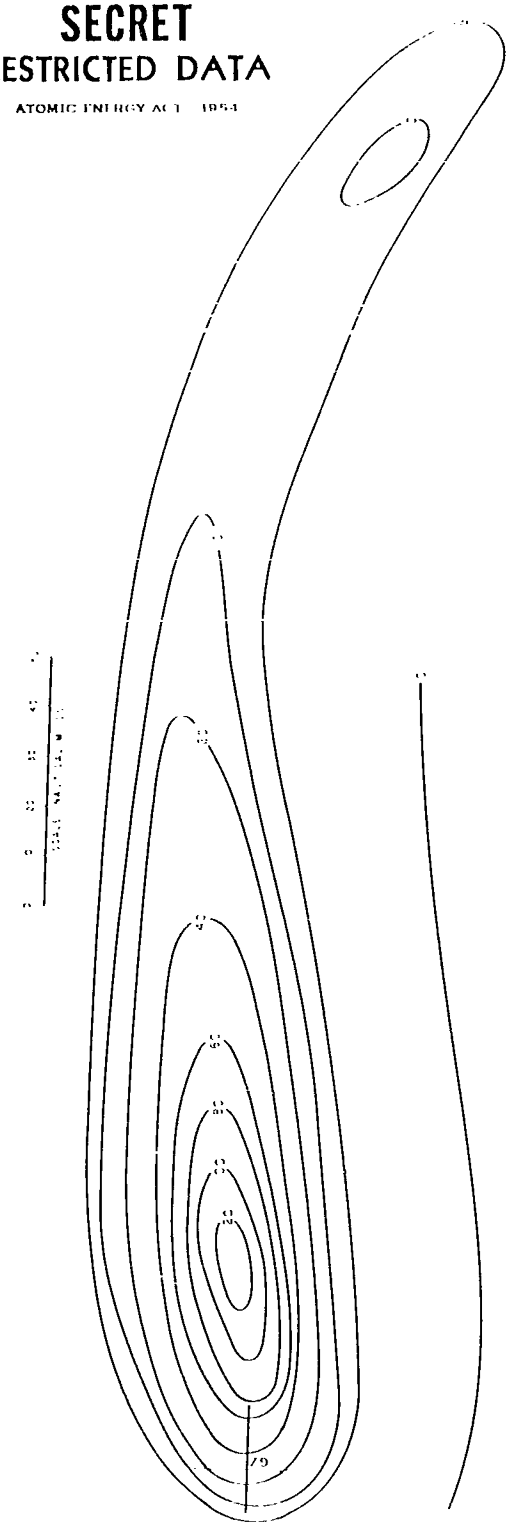

Fig. A-1—Run Ia, results of calculation
(Fraction of device/Kft X 10^7)

SECRET

for run 1b. Figure A2 shows the fallout computation for run 1b with isopleths subjectively drawn.

Table A4

$A_1(r)$ for Run 1b as a Function of (r),
and the Difference between A_1 for Run 1a and A_1 for Run 1b

Index	r	$A_1^b(r)$	$A_1^a - A_1^b$
1	9.5	.280	-.13
6	12.25	.389	-.15
11	15.0	.520	-.19
16	20.0	.648	-.24
21	24.0	.767	-.11
26	31.0	.865	.07
31	38.0	.918	.21
36	49.0	.928	.44
41	60.0	.883	.54
46	77.5	.800	.61
51	95.0	.685	.00
56	123.0	.559	-.13
61	151.0	.427	-.16
66	195.0	.310	-.12
71	239.0	.214	-.01
76	309.0	.140	.02
81	379.0	.086	.02
86	489.0	.051	.01
91	600.0	.028	.03

Run 1c

In order to be able to check the effect of the A(R) and A(H) distributions a model was set up which was similar to the model discussed in reference (1). The exponential decrease with height was assumed for the mushroom and the invariant distribution with R was retained. However 97 per cent of the activity was put into the mushroom, instead of 90 per cent as in the earlier model, and the remaining 3 per cent was used to make up run 1d. The input values are shown in Table A5 and the final pattern is shown in Fig. (A3).

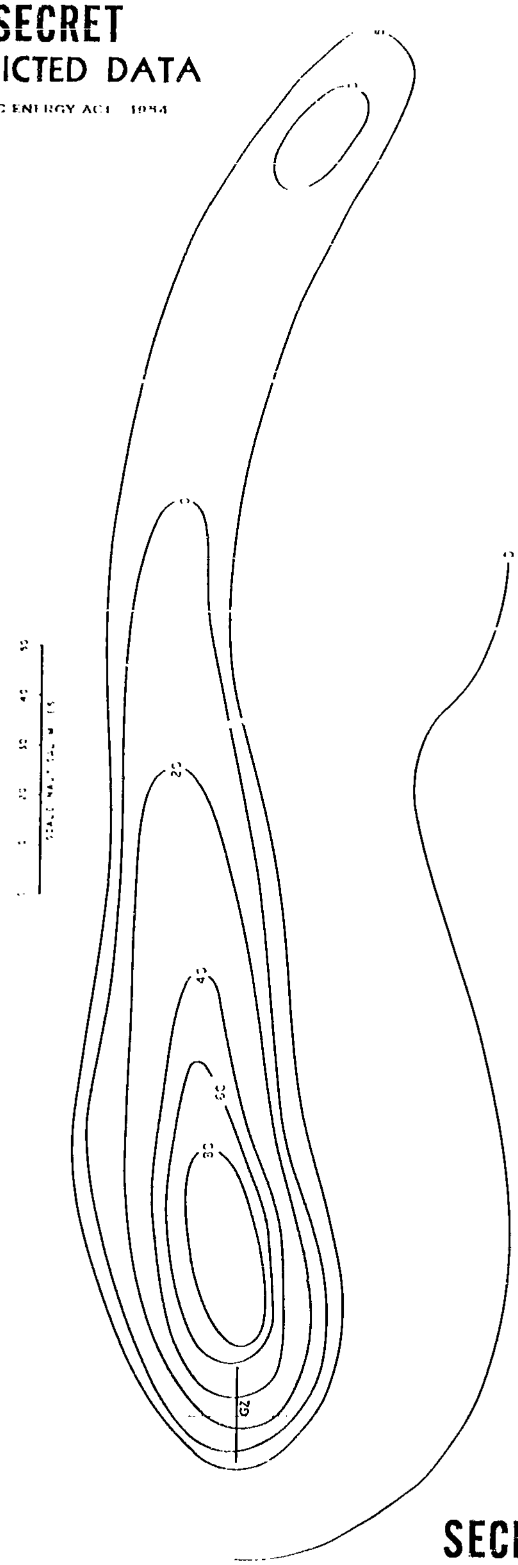

Fig. A-2—Run Ib, results of calculations
(Fraction of device/Kft X 10^7)

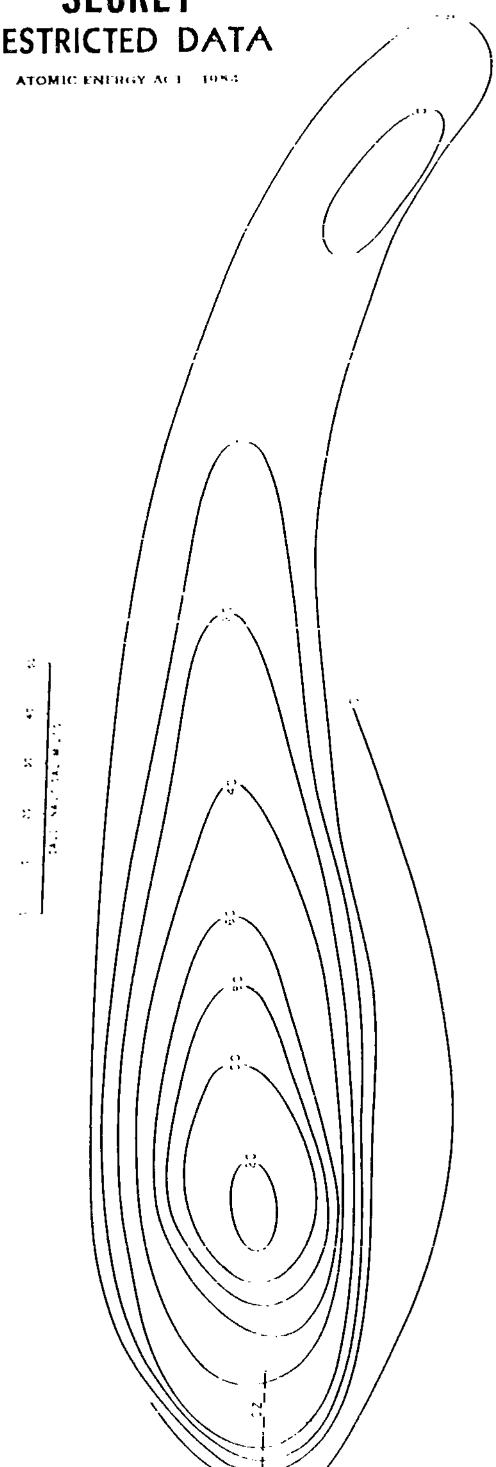

Fig. A-3—Run ic, results of calculations
(Fraction of device/Kft X 10^7)

Table A5

Activity Distribution for Run 1c

r	$A_1(r)$	R	$A_3(R)$	h	$A_2(H)$
9.5	0.1455	0	3.513×10^{-5}	0	0
12.25	0.2328	.822	3.513×10^{-5}	5	0
15.0	0.3201	1.645	3.513×10^{-5}	10	0
20.0	0.3977	2.467	3.513×10^{-5}	15	0
24.0	0.6402	2.467	3.513×10^{-5}	20	0
31.0	0.9021	2.467	3.513×10^{-5}	25	0
38.0	1.1543	2.467	3.513×10^{-5}	30	0
49.0	1.3289	2.467	3.513×10^{-5}	35	0
60.0	1.3774	2.467	3.513×10^{-5}	40	0
77.5	1.3677	2.467	3.513×10^{-5}	45	0
95.0	0.6596	2.467	3.513×10^{-5}	50	0
123.0	0.4171	2.467	3.513×10^{-5}	55	0.00560
151.0	0.2619	2.467	3.513×10^{-5}	60	0.04394
195.0	0.1843	2.467	3.513×10^{-5}	65	0.03472
239.0	0.1940	19.737	3.513×10^{-5}	70	0.02743
309.0	0.1552	20.557	0	75	0.02167
379.0	0.1067	20.557	0	80	0.01712
489.0	0.0582	20.557	0	85	0.01353
600.0	0	20.557	0	90	0.01069
		23.849	0	95	0.0084
				100	0.0067

Run 1d

This run was merely the stem portion of run 1c. The total fraction placed in the stem was only 3 per cent, and the addition of this fallout to run 1c made only minor changes in the pattern. In order to get the gross effects of the fallout, it appears unnecessary to be concerned with the stem. In fact even this small amount of stem fallout seemed to increase the error in the pattern in those areas wherein it was detectable.

Run 1e

This computation was designed to make a more radical change in the distribution function in order to produce a greater change in the pattern. Since the previous attempts indicated that there was too much debris too close to ground zero, the activity on the larger particles was drastically reduced. The activity size distribution of run 1e is shown in Table A6 and the resulting pattern is shown in Fig. (A4). It may be noted that the activity is spread further down-wind than in the other runs, although the maximum has been considerably lowered.

Table A6

The Function $A_1(r)$ for Run 1e

Index	r	$A_1(r)$
1	9.5	0.15
6	12.25	0.24
11	15.0	0.33
16	20.0	0.41
21	24.0	0.66
26	31.0	0.93
31	38.0	1.59
36	49.0	1.77
41	60.0	1.56
46	77.5	1.31
51	95.0	0.34
56	123.0	0.22
61	151.0	0.13
66	195.0	0.10
71	239.0	0.09
76	309.0	0.08
81	379.0	0.05
86	489.0	0.03
91	600.0	0

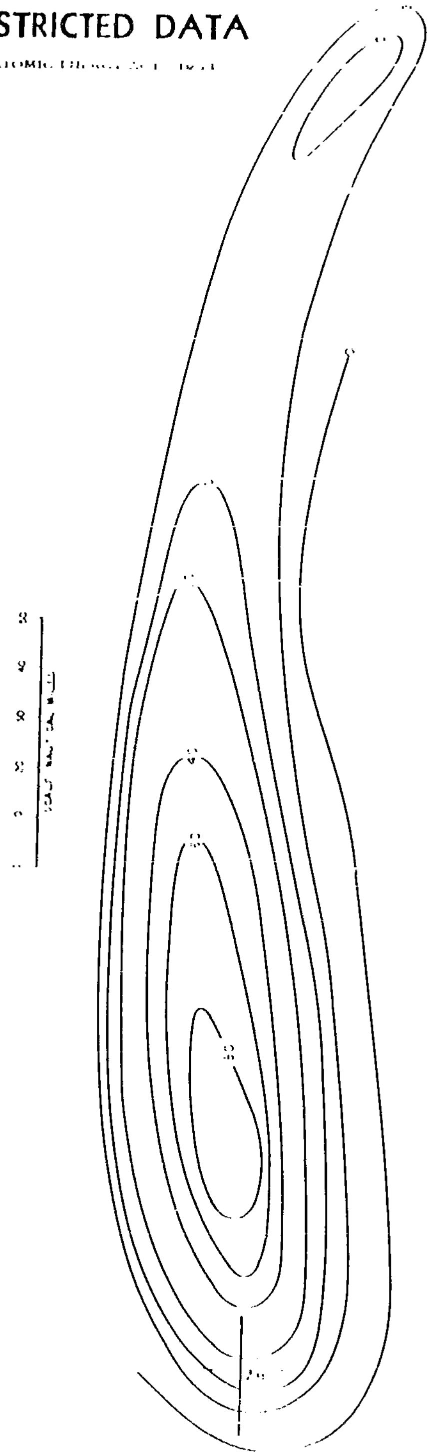

Fig. A-4 — Run Ie, results of calculations
(Fraction of device/Kft $X 10^{7}$)

REFERENCES

1. Greenfield, S. M., and R. R. Rapp, Fallout Computations and Castle-Bravo – A Case Study(U), Research Memorandum RM-1855, The RAND Corporation, January, 1957, (Secret Restricted Data).

2. Dishington, R. H., A Model for Fallout Calculations(U), Research Memorandum RM-1371, The RAND Corporation, October, 1954, (Confidential).

3. Greenfield, S. M., W. W. Kellogg, F. J. Krieger, and R. R. Rapp, Transport and Early Deposition of Radioactive Debris–Project Aureole(U), Report R-265-AEC, The RAND Corporation, July, 1954, (Secret Restricted Data).

4. AFSWP, 895, Fallout Symposium, Armed Forces Special Weapons Project, January, 1955, (Secret Restricted Data).

5. Rapp, R. R., and J. D. Sartor, Rate of Fall through the Atmosphere of Irregularly Shaped Particles, Research Memorandum RM-2006, The RAND Corporation, November, 1957, (Unclassified).

6. Rapp, R. R., The Vertical Transport of Particulate Matter through the Atmosphere, (To Be Published).

7. Schuert, E. A., "Employment of Time and Space Variable Winds Including Vertical Motions on the Analysis of Particle Trajectories, Appendix E in RAND Fallout Symposium," S-62, April, 1957, (Secret, formerly Restricted Data).

8. Dean, G. A., and W. D. Olmstead, An Example of Three Dimensional Analysis of the Wind Field over the Marshall Islands, Oahu Research Center Institute of Geophysics, University of California, 1954, (Official Use Only).

9. Van Lindt, V.A.J., L. E. Killian, J. A. Chiment, and D. C. Campbell, "Fallout Studies during Operation Redwing," ITR-1354, October, 1956, (Secret Restricted Data).

10. Kellogg, W. W., "Atomic Cloud Height as a Function of Yield and Meteorology," Paper P-881-AEC, The RAND Corporation, June, 1956.